Tikrit Journal of Engineering Sciences (2024); 31(2): 159-167
DOI: http://doi.org/10.25130/tjes.31.2.15

IRAQI Academic Scientific Journals

ISSN: 1813-162X (Print); 2312-7589 (Online)
Tikrit Journal of Engineering Sciences
available online at: http://www.tj-es.com

TJES Tikrit Journal of Engineering Sciences

Concrete Cover Effects on Longitudinal Steel Bars Corrosion Rates in Reinforced High-Performance Concrete Circular Short Columns

Lubna B. Mahmood *, Assim M. Lateef
Civil Engineering Department, Engineering College, Tikrit University, Tikrit, Iraq.

Keywords:
High-Performance Concrete (HPC); Corrosion; Clear Cover; Short Columns.

Highlights:

- Effect of corrosion on longitudinal steel bars in short columns.
- Effect of concrete cover on corrosion rate in short columns.
- High-performance concrete was used.
- Cross-section area and Weight losses due to corrosion in steel bars were estimated.

ARTICLE INFO
Article history:

Received	08 Apr.	2023
Received in revised form	09 May	2023
Accepted	19 June	2023
Final Proofreading	30 July	2023
Available online	20 May	2024

Citation: Mahmood LB, Lateef AM. **Concrete Cover Effects on Longitudinal Steel Bars Corrosion Rates in Reinforced High-Performance Concrete Circular Short Columns**. *Tikrit Journal of Engineering Sciences* 2024; **31**(2): 159-167.
http://doi.org/10.25130/tjes.31.2.15

*Corresponding author:
Lubna B. Mahmood
Civil Engineering Department, Engineering College, Tikrit University, Tikrit, Iraq.

Abstract: The main objective of this research is to investigate the concrete cover thickness effect on the corrosion degree of the longitudinal reinforcing steel of short circular high-performance concrete columns. The practical program consists of casting and testing six circular columns with dimensions of (150 × 1000) mm tested under a central load. Three of them were reference columns, and three were corroded using an accelerated corrosion cell. The main variable adopted in the present research included the concrete cover thickness (10, 20, and 30) mm to compare results for weight and surface area loss of corroded steel and bearing capacity reduction among all samples. The results showed that increasing the concrete cover thickness from 10 to 20 and 30 mm decreased the loss percentage of the reinforcing steel weight by (12.47, 11.82, and 11.26) %, respectively. Also, the loss percentage of the cross-sectional area of the reinforcing steel decreased by (77.44, 64.00, and 57.75) %, respectively. While bearing capacity was reduced by (29.07, 25.25, and 32.23) % for 10, 20, and 30 mm clear covers, respectively, compared with the control columns of 10, 20, and 30 mm clear covers.

تأثير سمك الغطاء الخرساني على درجة تآكل حديد التسليح الطولي في أعمدة الخرسانة عالية الأداء الدائرية القصيرة

لبنى براء محمود، عاصم محمد لطيف

قسم الهندسة المدنية/ كلية الهندسة / جامعة تكريت/ تكريت - العراق.

الخلاصة

الهدف الرئيسي من هذا البحث هو التحري عن تأثير سمك الغطاء الخرساني على درجة تآكل حديد التسليح الطولي (الرئيسي) لأعمدة الخرسانة عالية الأداء الدائرية القصيرة، البرنامج العملي يتألف من ست أعمدة بأبعاد (١٥٠×١٠٠٠) ملم، ثلاثة منها أعمدة مرجعية وثلاثة أعمدة معرضة للتآكل فحصت تحت تأثير حمل مركزي، شملت المتغيرات الرئيسية المعتمدة في البحث الحالي سمك الغطاء الخرساني (١٠، ٢٠، ٣٠) ملم، المقارنة بالنتائج بين جميع العينات على مقدار الفقدان في وزن الحديد المتآكل ومقدار الفقدان في المساحة السطحية للحديد المتآكل ومقدار النقصان في قابلية تحمل الاعمدة. خلال الفحص العملي أوضحت النتائج بأنه بزيادة سمك الغطاء الخرساني تقل نسبة الفقدان بوزن حديد التسليح بمقدار (١٢,٤٧، ١١,٨٢، ١١,٢٦) ونسبة الفقدان بمساحة المقطع العرضي له بمقدار (٧٧,٤٤، ٦٤,٠٠، ٥٧,٧٥) %. بينما قلت قابلية تحمل الاعمدة بمقدار (٢٩,٠٧، ٢٥,٢٥، ٣٢,٢٣) % للأعمدة ذات الغطاء الخرساني ١٠، ٢٠، و٣٠ ملم على التوالي، مقارنة بالعامود المرجع.

الكلمات الدالة: خرسانة عالية الاداء، التآكل، الغطاء الخرساني، الاعمدة القصيرة.

1.INTRODUCTION

In concrete, steel is generally protected from corrosion by the highly alkaline environment created around it. The interface between steel and concrete generates a passive layer of iron oxides, acting as a barrier against corrosion. However, any residual corrosion or cracks in the concrete surface accelerates the corrosion rate, as the volume occupied by the corrosion products is approximately six times larger than the original steel [1]. Corrosion is a major problem affecting reinforced concrete structures' durability and serviceability. It occurs due to the reaction between the steel reinforcement and the surrounding environment, such as moisture, oxygen, and chemical substances. The corrosion process can cause cracking, spalling, and loss of structural integrity, ultimately leading to the structure's failure. Factors that can influence corrosion include the presence of chlorides, carbonation, pH level, and exposure to aggressive environments. Preventive measures include proper design and construction techniques, selecting appropriate materials, regular maintenance and inspection, and using protective coatings and cathodic protection systems [2]. There are two main categories of corrosion that can occur on a steel bar in reinforced concrete, i.e., generalized and localized. Pitting corrosion, also known as localized corrosion, is characterized by isolated pits forming along the steel bars. In contrast, generalized corrosion spreads uniformly along the steel bar [3]. It is crucial to note that the passive layer stability is influenced by the concrete quality and the thickness of the concrete covering the steel reinforcement. They affect the system's capacity to exclude aggressive chemicals, which tend to change the pore water composition in ways that threaten the passivity of embedded steel and hence lead to substantial corrosion [4]. Ahmed [5] reported that the capacity of steel bars to carry stress was reduced due to the loss of cross-sectional area. Meanwhile, Shayanfar et al. [6] found that concrete with wider and more uniform grains and a lower water-cement ratio (resulting in higher compressive strength) exhibited lower levels of corrosion. However, when the corrosion degree increased, the compressive strength decreased. Hodhod and Ahmed [7] examined the Artificial Neural Network (ANN) as an alternative technique to model the beginning of corrosion in slag concrete. The selected network architecture had four neurons in the input layer that represent the values of the concrete cover depth, apparent chloride diffusion coefficient, chloride threshold value, and surface chloride concentration. One neuron in the output layer represented the corresponding corrosion initiation time value. The investigation's results clearly showed that the corrosion start time increased with deeper concrete covers, lowered with higher surface chloride concentrations, and increased with lower chloride diffusion coefficients. When the chloride threshold value increased, the corrosion onset time increased. To ascertain the lifetime of reinforced concrete structures in connection to chloride permeability, concrete cover, and the curing process, Tahershamsi [8] carried out an empirical and experimental investigation. Ten different curing methods were used to examine the corrosion resistance of samples of reinforced concrete that had been treated with a 5% NaCl solution. The investigation was divided into two sections: an accelerated corrosion test on 80 concrete prisms implanted with a steel bar, and tests on the compressive strength and chloride permeability of 50 concrete cylinders. A DC power supply was used to power the samples, and the cathode (-) served as the anode (+). The samples were connected in parallel to maintain a constant voltage of 12 V. The specimens were monitored for the onset of corrosion, cracking, and damage while fully immersed in a 5% sodium chloride solution. According to the results, samples with greater chloride permeability and lower concrete cover had initiation periods as short as 1 day and extended to 53 days. The

concrete cover had a significant impact on the onset time of corrosion; For 20 mm, 30 mm, 40 mm, and 60 mm coverslips, respectively, initiation times were 1.5, 5, 14, and 37 days. Cracking time was postponed by increasing the concrete cover from 20mm to 60mm; The corresponding median cover durations were 3, 9, 18, and 43 days. Linear polarization method was used in the study of Loreto et al. [9] The to examine the corrosion rate of steel bars in reinforced concrete. They also investigated the relationship between concrete crack width, corrosion rate, and residual strength. The expected service life of the concrete cover was estimated by taking into account variables such as the length of the starting stage, the penetration rate of the aggressive agent, and the depth of the cover. In order to determine cover depth, expected exposure was taken into account during the design phase. The tensile strength of the specimens, fracture depth, and corrosion rate were evaluated using accelerated aging. The tensile strength of the concrete cover was confirmed using a separate tensile test, often known as the Brazilian test. Concrete diffusivity (Dapp) was used to calculate the commencement and propagation durations, which yielded the residual service life. In order to evaluate the durability of concrete, accelerated corrosion experiments were carried out. The findings were compared with data from the literature, demonstrating the superior resistance of pozzolan cement to chloride penetration. The study discovered that tensile strength declined with increasing fracture breadth, which was correlated with the rate of corrosion. Additionally, the study contrasted the outcomes of accelerated tests with those of natural exposure, providing insightful information on contrasting laboratory work with real-world exposure. According to the projection study, a 25-year service life start time may be attained by increasing the cover thickness and Dapp. Mahmood and Lateef [10] investigated the effect of corrosion on longitudinal steel bars in reinforced concrete beams and how this affects the flexural strength of beams. The researchers used reinforced concrete beams in their experimental study, and the degree of corrosion of the steel bars varied. The results showed that corrosion significantly reduced the flexural strength of the beams, with the amount of corrosion affecting the strength loss. Our knowledge of how corrosion affects reinforced concrete structures has improved as a result of this work. The need to mitigate and prevent corrosion in maintaining the structural integrity of reinforced concrete components has been brought to the attention of engineers and industry professionals. Al-Hazragi and Lateef [11] examined the behavior of uniaxially reinforced concrete columns reinforced with fiber-reinforced polymers (FRP) and ultra-high-performance concrete (UHPC). The authors used reinforced concrete columns reinforced with FRP and UHPC to conduct an experimental analysis. The load-bearing capacity and ductility of reinforced concrete columns were found to be significantly increased by combining UHPC and FRP, according to the results. The study added to our understanding of how reinforced concrete structures can be strengthened and retrofitted using advanced materials and methods. The results of this research can provide important perspectives for engineers and professionals in creating and implementing effective fortification plans for existing constructions.

2.EXPERIMENTAL METHOD

2.1.Materials

In this study, the high-performance concrete (HPC) mix was employed. A detailed summary of the materials utilized is provided in Table 1. Deformed rebar used 6mm and 8mm nominal diameter reinforcing steel rods. The bar's characteristics matching the ASTM A615 standards [12] are displayed in Table 2.

Table 1 Description of Materials.

Material	Descriptions
Cement	Mass Factory's Type I ordinary Portland cement is consistent with Iraq's Iraqi Specification No. 5/1984. [13]
Quartz Sand	Quartz sand with a maximum size of 600μm and compatible with the B.S. specification No.882/1992 [14]
Silica Fume	A highly active pozzolanic substance made up of very small, spherical particles known as micro-silica (BASF MasterRoc MS610) is compatible with the ASTM C 494/C494M-17 [15]
Super Plasticizer	The admixture BASF MasterGlenium 51 (Advanced Polycarboxylate Super Plasticizer) was used and compatible with the ASTM C494, 2013 [16]
Water	pristine tap water (used for mixing and curing)
Steel Bars	Deformed steel bars with a diameter of 8 and 6 mm

Table 2 Steel Bar Reinforcement Test Results.

Bar diameter (mm)	Measured diameter (mm)	Yield stress *fy* (MPa)	Ultimate stress *fu* (MPa)	Elongation %
6	5.6	430	568.80	6.1
8	8	450	625.88	7.3

2.2.Columns Specimens Design and Details

According to ACI 318-14, ρ should be not less than 0.01 or greater than 0.08. First, check the column dimension required for minimum steel (ρ = 0.01, 6 longitudinal steel bars of 8 mm, and spiral of 6 mm with 75 mm spacing). The cross-section of each specimen was 150 mm in diameter by 1000 mm in height, with three distinct clear cover thicknesses (10, 20, and 30 mm). 6 Ø8 mm steel bars were used as the main longitudinal reinforcement, and spiral stirrups of Ø6 mm steel bars at 75 mm spacing. The reinforced concrete columns tested in this study are illustrated in Fig. 1.

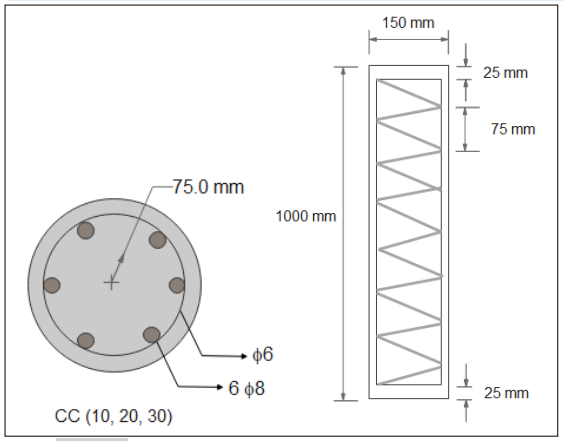

Fig. 1 Dimensions and Reinforcement Specifics of the Tested Columns.

2.3.Experimental Program

Six circular short-column specimens of a dimension of (150 × 1000) mm with different clear cover thicknesses of 10, 20, and 30 mm were cast and tested, two columns for each clear cover thickness. Three columns were adopted as control columns, whereas three columns subjected to corrosion (longitudinal steel bars) for 20 days were tested as part of the experimental program. The entire details about the tested columns are included in Table 3.

Table 3 General Information and the Tested Column's Variables.

Column Symbol	Type of Column	Clear Cover Thickness (mm)
H.R.10	Control Column	10
H.R.20	Control Column	20
H.R.30	Control Column	30
H.C.L.10	Corroded Column	10
H.C.L.20	Corroded Column	20
H.C.L.30	Corroded Column	30

2.4.Cover Blocks and Electrical Insulation

A cover block was used as a spacer for the columns. It was made of 10, 20, and 30 mm cement mortar. Small plastic water pipes were used as a mold for the blocks. Small thin water pipes were used as electrical insulations to insulate the longitudinal steel bars and stirrups for the samples that studied the corrosion for one part of the reinforcements. Fig. 2 shows the cover blocks and the electrical insulation.

(a) Electrical Insulation. **(b)** Cover Block.

Fig. 2 The Cover Blocks and Electrical Insulation.

2.5.Concrete Mix Design

In this study, the material mix proportion listed in Table 4 was employed for 80 MPa compressive strength. Using a flow table test per ASTM C1437-01 [17], the workability of the typical concrete mix was evaluated.

Table 4 Mix Proportion.

Ingredient	Cement	Quartz Sand	Silica	SP %	W/C ratio
Quantities (kg/m³)	1000	1000	100	1.8	0.22

2.6.Concrete Mixing and Curing

For the concrete mix to have the necessary workability and homogeneity, the mixing process is crucial. An electric mixer was used to help with the mixing procedure. The casting specimen is displayed in Fig.3. The following mixing technique has been advised by Mahmood and Lateef [10]:

1. Preparing and weighing the materials for the mixture (Cement, Quartz Sand, Silica Fume, Super Plasticizer, and Water)
2. Water is used to moisten the mixer basin to prevent water in the mixture from absorbing and changing the mixture ratios.
3. Quartz sand was added to the mixer for 1 minute.
4. The silica fume and cement were mixed in a dry condition to disperse the silica fume particles throughout the cement particles for 5 minutes.
5. Superplasticizer was added to the water and stirred, then added to the dry mix in three batches for 3 minutes.
6. The mixer was switched off to clean the edges of the mixer, and continued the mixing process for 5 minutes.
7. The mixing process continued for 16 minutes.

Fig. 3 Casting of HPC Columns.

2.7.High-Performance Concrete (HPC) Mechanical Properties

To evaluate the concrete mix's mechanical properties, the control specimens were mixed and cast. The compression strength and splitting strength were determined by testing

three cubes (100mm×100mm×100mm) according to BC 1881- part 116 [18] and three cylinders (100mm × 200 mm) according to ASTM C494-M04 [16]. The corresponding results can be found in Table 5.

Table 5 Concrete Mix Mechanical Characteristics on Day 28.

Compressive Strength f_{cu} (MPa)	Splitting Tensile Strength f_{ct} (MPa)
80	7

2.8.Corrosion Cell

The accelerated corrosion method described by Li et al. [19] was employed in this study for twenty days, with a current density of one milliampere per cubic centimeter. To supply current to the specimens in the corrosion basin, a dual power supply model (PS 303-2) with a maximum current of 3A and a voltage of 30V was used, given the sample size (surface area for longitudinal steel bars) used in the study. The anode electrode consisted of eight longitudinal steel bars per column, while a stainless-steel plate served as the cathode electrode beneath each column. Pure salt (NaCl) was added to the basin at a ratio of 5% of its volume. Fig. 4 depicts the corrosion cell used in the study and a corroded column.

(a) The Corrosion Cell During Operation.

(b) Corroded Column.

Fig. 4 Corrosion Process.

2.9.Columns Test

To begin the testing, the designated column was placed into the testing device, and then the LVDT was installed beside it. A cylindrical roller was used to apply the linear load, a support plate was used for axially loading the specimens, and the support condition was pinned-pinned. The load was incrementally increased, with readings taken at 5.0 kN intervals until the column failed. The vertical LVDT, which could move from bottom to top, was used to measure the axial deformation of the columns under load. The longitudinal strains were measured with a strain gauge. Each load increase was recorded, as depicted in Fig 5. Fig. 6 shows the tested columns.

2.10.Determination of Corrosion

Following the testing and failure of the damaged columns, the corroded reinforcing steel bars were cleaned using kerosene oil to eliminate any rust particles. To determine the amount of corrosion that occurred in the steel bars, two techniques were employed, namely the weight loss method and the loss in the cross-sectional area. These techniques were adopted by Li et al. [19], and the results are presented in Table 6.

Table 6 Test Results of Column Specimens.

Column Symbol	Loads (KN)	Steel Bar Weight (g)	Steel bar Sectional Area (mm2)
H.R.10	950.62	195.00	50.27
H.R.20	889.66	195.00	50.27
H.R.30	742.54	195.00	50.27
H.C.L.10	674.28	170.69	11.34
H.C.L.20	664.99	171.96	18.10
H.C.L.30	503.22	173.05	21.24

2.10.1.Weight Loss Percentage

The weight loss method was employed to determine the corrosion loss of the steel bars. This method involves measuring the weight of the bars before and after the corrosion process and then calculating the percentage weight loss using Eq. (1):

$$\omega\% = \frac{w1-w2}{w1} \times 100\% \qquad (1)$$

where w_1 and w_2 represent the weights of steel bars before and after corrosion, respectively.

2.10.2.Sectional Area Loss

To determine the loss of cross-sectional area for steel bars before and after corrosion, the average diameter was measured at six different locations on each steel bar, following Li et al. [19]. The area of each average diameter was then calculated.

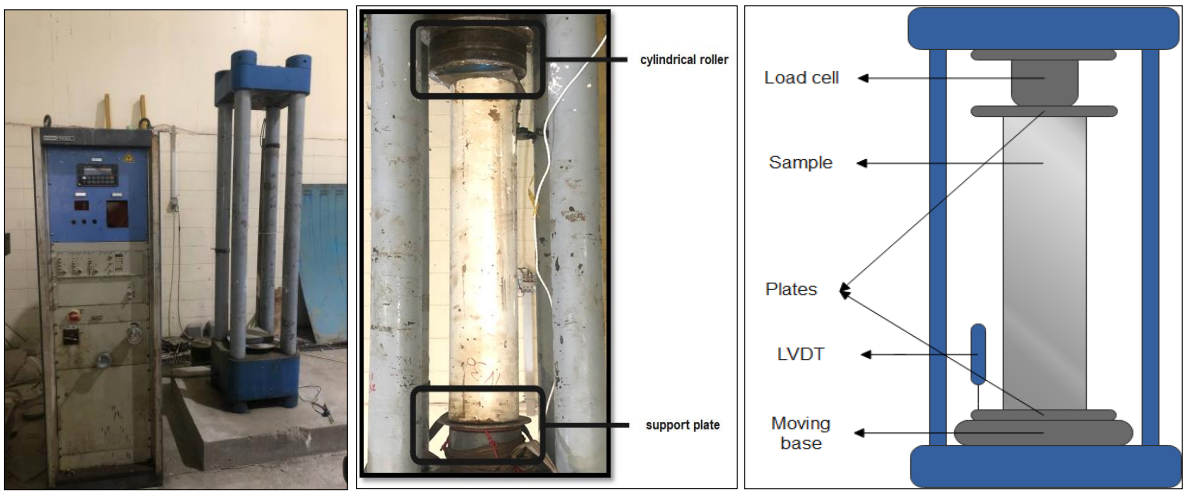

(a) The testing Device **(b)** Sample while testing. **(c)** Test setup

Fig.5 Testing Device.

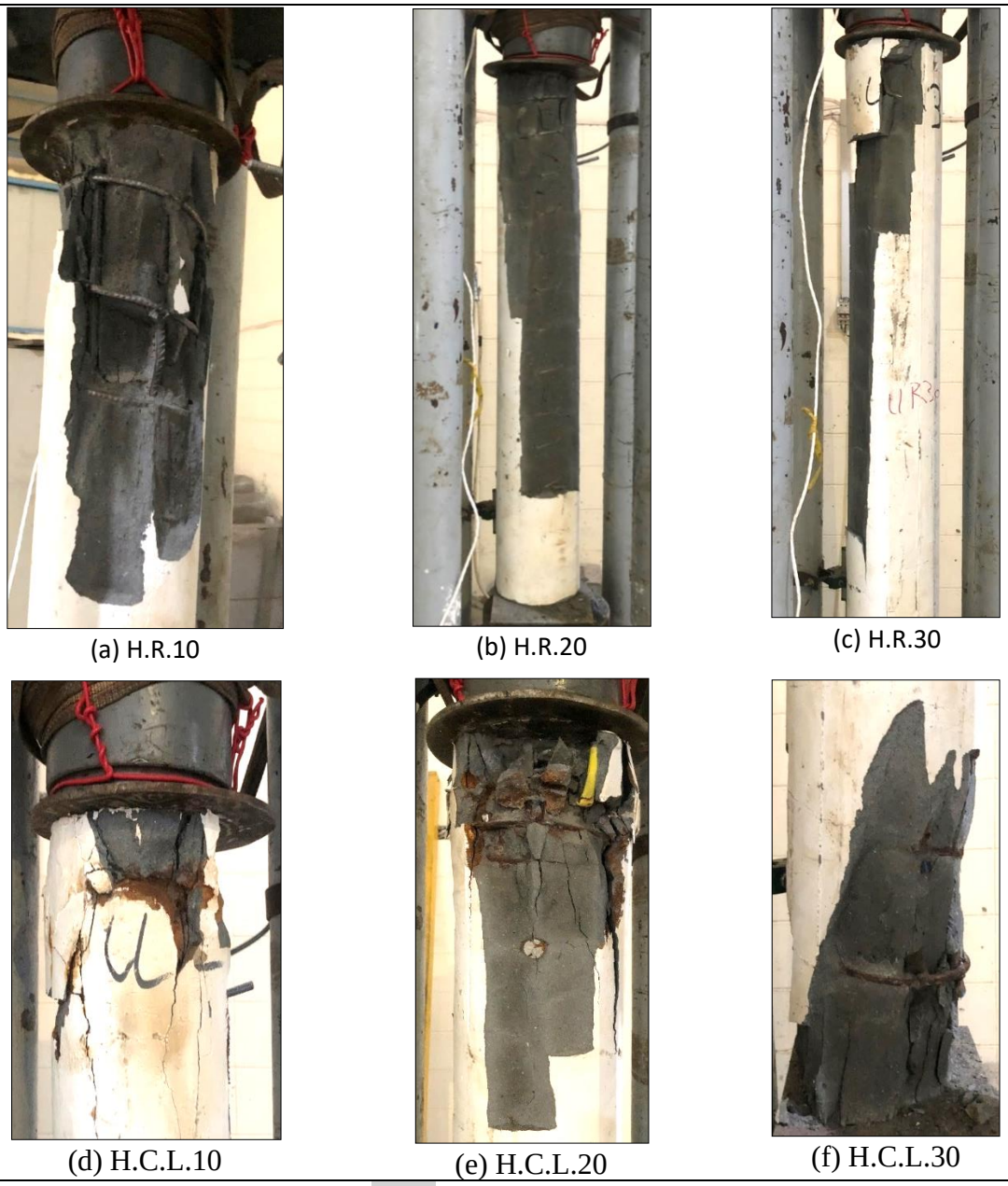

(a) H.R.10 (b) H.R.20 (c) H.R.30

(d) H.C.L.10 (e) H.C.L.20 (f) H.C.L.30

Fig.6 Tested Columns.

3.RESULTS AND DISCUSSION

The transparent cover thicknesses' effects on corrosion degree by estimated weight loss % and sectional area loss were tested on control and corroded reinforced concrete column specimens during the experimental program. The test outcomes are displayed in Table 6.

3.1.Ultimate Loads

The test was conducted on all column specimens until failure occurred. The ultimate loads of the tested columns have been documented and are found in Table 6. The results indicated that the corroded samples' ultimate loads with clear cover thicknesses of 10 mm, 20 mm, and 30 mm decreased by approximately 29.07%, 25.25%, and 32.23%, respectively, compared to the control columns, due to the corrosion damage, as illustrated in Fig. 7.

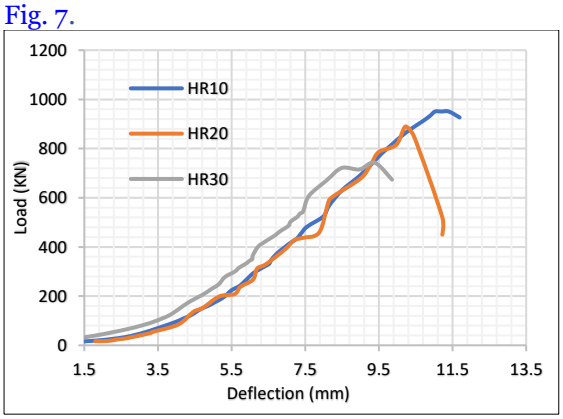

(a) Load-Deflection Curves for Control Columns.

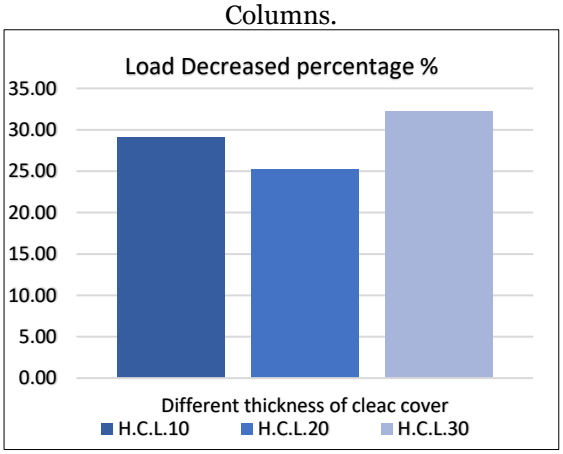

(b) Load Decrees Percentage for Corroded Columns.

Fig. 7 Ultimate Loads Results.

3.2.Weight Loss Percentage %

Fig. 8 displays the weight loss percentage of longitudinal reinforcement steel bars for clear cover thicknesses of 10, 20, and 30 mm after the corrosion process, which reduced by 12.47, 11.82, and 11.26 %, respectively, compared to the control columns. The weight of corroded steel columns is presented in Table 6 relative to the weight of the original steel bars before exposure to corrosion. Additionally, the 10 mm thickness cover exhibited cracking during the corrosion period, as shown in Fig. 9.

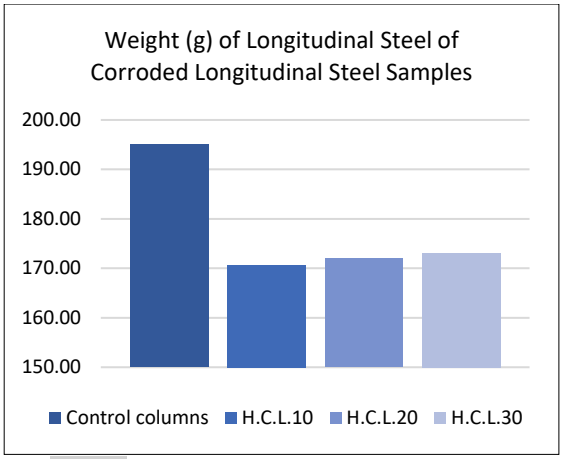

Fig. 8 Losses of the Steel Bar's Weight.

Fig. 9 10 mm Cover Cracking.

3.3.Sectional Area Loss

The reduction in the cross-sectional area of steel bars after the corrosion process was measured for clear cover thicknesses of 10, 20, and 30 mm. The results in Table 6 indicated a decrease compared to the control columns. Specifically, the cross-sectional loss percentage decreased by 77.44, 64.00, and 57.75 % for the respective thicknesses, as depicted in Fig. 10. A corroded steel bar is also shown in Fig. 11.

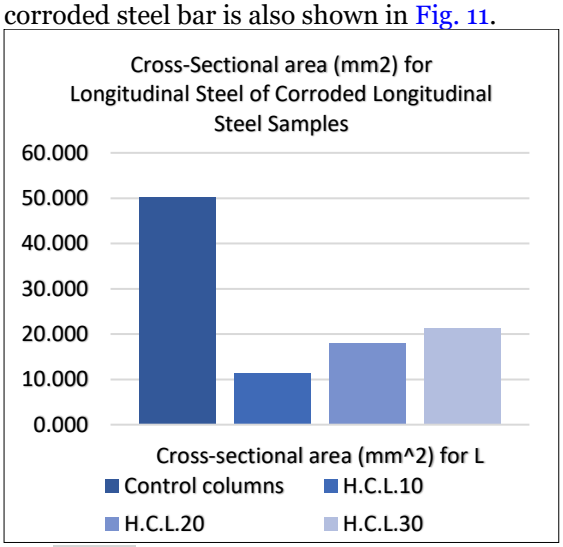

Fig.10 Losses in Cross-Sectional Area.

Fig.11 Corroded Steel Bar.

4.CONCLUSIONS

The experimental findings lead to the following conclusions:

1. Initially, it can be observed that the ultimate loads of corroded HPC columns decreased with the control columns due to the corrosion process, with a decrease of 29.07% and 25.25% for clear cover thicknesses of 10 mm and 20 mm, respectively. The reduction in load for the sample of 20mm cover was less than that of the sample of 10mm cover because the latter caused more corrosion to the column. As a result, the reduction rate in load was higher for the sample of 10 mm cover.
2. The 30 mm clear cover column had a lower load-bearing capacity than the other two covers (20 and 10) mm because the 30 mm clear cover reduced the effective diameter of the column, i.e., the amount of concrete available to resist the compressive stresses, more than the smaller clear covers resulting in a decrease in the column's compressive strength by reducing the amount of concrete available to resist the compressive stresses. ACI 318-14 specifies that the reduction in the effective area of concrete due to the clear cover (d) can be calculated using equation in ACI code index with no. (7.7.3), where:

$$d = C_{min} + (\emptyset/2) + (\emptyset_{sp}/2) + (\emptyset_{sp,max}/2) - \emptyset$$

The reduction in the nominal axial strength due to the reduction in the effective area of concrete can be calculated using equation in ACI code index with no. (7.7.4), where:

$$P_n,d = 0.85fc'A'g + A_{st}f_y$$

3. The accelerated corrosion process application resulted in a reduction of the weight of steel bars by 12.47, 11.82, and 11.26 % and a decrease in the cross-sectional area of longitudinal steel bars by 77.44, 64.00, and 57.75 % for clear cover thicknesses of 10, 20, and 30 mm, respectively.
4. The results of the loss in the weight of the reinforcing steel and its cross-sectional area, and after comparing them, showed that the concrete cover thickness was inversely proportional to the reinforcing steel corrosion degree, where the greater the thickness of the concrete cover, the less the effect of corrosion because the concrete cover represented the path that water and materials followed. Corrosive up to the reinforcing steel, where the greater this path, the less severe the impact of the reinforcing steel, considering maintaining the column effective diameter within acceptable limits to preserve the bearing capacity of the column as much as possible.

REFERENCES

[1] Broomfield J. **Corrosion of Steel in Concrete: Understanding, Investigation and Repair**. Abingdon: United Kingdom: Taylor & Francis; 2003.

[2] Rodrigues R, Gaboreau S, Gance J, Ignatiadis I, Betelu S. **Reinforced Concrete Structures: A Review of Corrosion Mechanisms and Advances in Electrical Methods for Corrosion Monitoring**. *Construction and Building Materials* 2021; **269**:121240, (1-83).

[3] Vavpetič P. Corrosion in Concrete Steel. Kamnik 2008:1-16.

[4] El-Reedy MA. **Steel-Reinforced Concrete Structures: Assessment and Repair of Corrosion**. 1st ed., Boca Raton: CRC Press; 2008.

[5] Ahmad S. **Residual Flexural Capacity of Corroded Reinforced Concrete Beams**. *IOP Conference Series: Materials Science and Engineering* 2018; **377**(1): 012121, (1-7).

[6] Shayanfar MA, Barkhordari MA, Ghanooni-Bagha M. **Effect of Longitudinal Rebar Corrosion on the Compressive Strength Reduction of Concrete in Reinforced Concrete Structure**. *Advances in Structural Engineering* 2016;**19**(6):897-907.

[7] Hodhod O, Ahmed H. **Modeling the Corrosion Initiation Time of Slag Concrete Using the Artificial Neural Network**. *HBRC Journal* 2014; **10**(3) :231-234.

[8] Tahershamsi M. ***Structural Effects of Reinforcement Corrosion in Concrete Structures***. Ph.D Thesis. Chalmers University of Technology; Gothenburg, Sweden: 2016.

[9] Loreto G, Di Benedetti M, Iovino R, Nanni A, Gonzalez MA. **Evaluation of Corrosion Effect in Reinforced Concrete by Chloride Exposure**. *Proceedings Volume 7983, Nondestructive Characterization for Composite Materials, Aerospace Engineering, Civil Infrastructure, and Homeland Security* 2011; Diego, California, United States : p. 119-128.

[10] Mahmood NK, Lateef AM. **Effect of Corrosion Longitudinal Steel Bars on the Flexural Strength of RC Beams**. *Tikrit Journal of Engineering Sciences* 2021;**28**(2):44-53.

[11] Al-Hazragi AASI, Lateef AM. **Behaviour of Uniaxial Reinforced Concrete Columns Strengthened with Ultra-High Performance Concrete and Fiber Reinforced Polymers**. *Tikrit Journal of Engineering Sciences* 2021;**28**(2):54-72.

[12] ASTM, A615/A615M-09. Standard Specification for Deformed and Plain Carbon-Steel Bars for Concrete Reinforcement. 2009.

[13] No.5/1984. Portland Cement. Iraqi Specifications 1984.

[14] B.S.882. Specifications for Aggregates from Natural Sources for Concrete British Standards Institute 1992.

[15] ASTM, C1240-03. Standard Specifications for Use of Silica Fume as a Mineral Admixture in Hydraulic –Cement Concrete, Mortar, and Grout. 2003.

[16] ASTM, C494/C494M. Standard Specification for Chemical Admixtures for Concrete. 2013.

[17] ASTM, C1437. Standard Test Method for Flow of Hydraulic Cement Pastes and Mortars of Plastic Consistency. 2001.

[18] BS1881, Part116. Method for Determination of Compressive Strength of Concrete Cubes. British Standards Institution 1989;3pp.

[19] Li H, Li B, Jin R, Li S, Yu J-G. **Effects of Sustained Loading and Corrosion on the Performance of Reinforced Concrete Beams**. *Construction and Building Materials* 2018; **169**:179-187.

[20] ASTM C 494/C494M-17. Standard Specifications for Chemical Admixtures for Concrete. 2017.